Surface biasing influence on the physical sputtering in fusion devices

2016 J. Phys.: Conf. Ser. 748 012002

(http://iopscience.iop.org/1742-6596/748/1/012002)

Surface biasing influence on the physical sputtering in fusion devices

I Borodkina[1,2], D Borodin[2], S Brezinsek[2], I V Tsvetkov[1], V A Kurnaev[1], C C Klepper[3], A Lasa[3], A Kreter[2] and JET Contributors*

EUROfusion Consortium, JET, Culham Science Centre, Abingdon, OX14 3DB, UK
[1]National Research Nuclear University MEPhI (Moscow Engineering Physics Institute), 31 Kashirskoe highway, Moscow 115409, Russia
[2]Forschungszentrum Jülich GmbH, Institut für Energie- und Klimaforschung - Plasmaphysik, Jülich 52425, Germany
[3]Oak Ridge National Laboratory, Oak Ridge, TN 37831-6169, USA
*See F. Romanelli et al., Proc. of the 25th IAEA Fusion Energy Conference 2014, Saint Petersburg, Russia

Corresponding author e-mail: ieborodkina@mephi.ru

Abstract. A new simplified analytical expression for the electromagnetic field in the Debye sheath in the presence of an oblique magnetic field including surface biasing effect is suggested. It is in good agreement with the numerical solution of the integral equation for the potential distribution in the Debye sheath. The energy and angular impact distributions and corresponding surface sputtering yields were analyzed in the presence of an oblique magnetic field and surface biasing. The analytical expression was used to estimate a) the effective sputtering yield of the W target with a varying negative voltage against plasma in PSI-2 linear device and b) erosion of the JET outer wall Be limiter near the ICRH antenna enhanced during RF emission.

1. Introduction

Understanding plasma-surface interaction (PSI) processes is important for the successful realization of the ITER project. PSI processes such as erosion and deposition lead to reduction of life time of plasma-facing components (PFC) in fusion devices. For correct calculation of the sputtering yields for PFCs in the presence of an oblique magnetic field the accurate expression for the sheath electric field must be included. Furthermore, in a number of experiments surface biasing (SB) up to several hundred Volts is applied to the PFC (e.g. to study the effect of ion impact energy influence), which also influences greatly the sheath potential distribution.

In the present paper the simplified analytical expression (AE) for the electromagnetic field suggested in [1] is updated to include the SB effect and an oblique magnetic field. Using this expression we reveal the influence of SB on the ion impact energy and angle distributions, which have strong influence on local physical sputtering yields.

The AE mentioned above was used to estimate the sputtering yield of the W target under Ar plasma exposure in PSI-2 linear plasma device [2]. In this experiment, the magnetic field is directed normal to the target surface. However, the additional negative SB of up to several hundred Volts (applied to the target to vary the sputtering ion energies) has a considerable influence on the sheath potential, the energy distributions, and thus, it must be treated as an additional parameter in the analytical solution.

In the case of modeling of PSI processes at the JET ITER-like wall (ILW), an oblique magnetic field is the most common scenario, and thus should be taken into account. The strong effect of the magnetic field angle in the energy and angle distributions highlights the relevance of the present effort in a correct estimate of sputtering yields. The suggested AE has been applied for modeling of radio-frequency (RF)-sheath enhanced erosion of the outer wall JET Be limiter near the Ion Cyclotron Resonance Heating (ICRH) antenna, aiming to improve the modeling presented in [3]. The comparison of the simulated RF-enhanced Be emission with experimental observations is presented.

2. Surface biasing influence on potential distribution in the sheath

The expression for the dependence of target potential on the SB was derived from the charge conservation law (similar to [4] (2.65)) where we take into account the difference in areas of target and return (surrounding) surfaces:

$$S_{rs} \cdot \Gamma^e_{rs} + S_t \cdot \Gamma^e_t = n_{se} c_s (S_t + S_{rs}) \tag{1}$$

where S_t, S_{rs} are the areas of the target and the return surface, Γ^e_t and Γ^e_{rs} are electron flux densities on the target and the return surfaces, n_{se} is plasma density at the sheath edge, c_s is the sound speed and $\Gamma^i = n_{se} c_s$ is the ion flux density on the surfaces. The electron flux densities reaching the target and return surfaces according to [4] are:

$$\Gamma^e_t = \frac{1}{4} n_{se} \overline{c_e} \exp\left[\frac{e(U_t - U_{pl})}{kT_e}\right] \tag{2}$$

$$\Gamma^e_{rs} = \frac{1}{4} n_{se} \overline{c_e} \exp(\frac{e(U_{rs} - U_{pl})}{kT_e}) \tag{3}$$

The ion flux density on the surfaces Γ^i is the same as without SB:

$$n_{se} c_s = \frac{1}{4} n_{se} \overline{c_e} \exp(\frac{eU_{sf}}{kT_e}) \tag{4}$$

where $\overline{c_e}$ is the thermal electron speed, U_{pl} is the plasma potential at the sheath/presheath boundary, U_{sf} is the surface floating potential relative to U_{pl} ([4] (2.60)), U_t is the target potential, U_{rs} is return surface potential.

Then, rewriting equation (1) in the following way,

$$\Gamma^e_t = \frac{n_{se} c_s}{\dfrac{S_t}{S_t + S_{rs}} + \dfrac{S_{rs}}{S_t + S_{rs}} \cdot \dfrac{\Gamma^e_{rs}}{\Gamma^e_t}} \tag{5}$$

we substitute equations (2)-(4) into (5) and obtain the expression for the dependence of target potential on the SB:

$$\frac{e\left(U_t - U_{pl}\right)}{kT_e} = \frac{e\left(U_{sf}\right)}{kT_e} - \ln\left[\frac{S_t}{S_t + S_{rs}} + \frac{S_{rs}}{S_t + S_{rs}} \exp\left(\frac{e\Delta U_{bias}}{kT_e}\right)\right] \tag{6}$$

where $\Delta U_{bias} = U_{rs} - U_t$ is a negative surface biasing.

As the area of the return surface is usually much larger than that of the target ($S_t << S_{rs}$), the target potential in the presence of SB can be calculated as:

$$\frac{e\left(U_t - U_{pl}\right)}{k \cdot T_e} = \frac{e\left(U_{sf}\right)}{kT_e} - \frac{e\Delta U_{bias}}{kT_e} \quad (7)$$

Further, PSI processes are determined to a large extent by the Debye sheath (DS) and magnetic pre-sheath (mps) effects, where the strong electric field is located. As the SB influences the potential distribution only in the DS [5], the analytical potential expression obtained in [1] can also be used here for the mps:

$$\psi(\xi) = \psi_{mps} \cdot \exp(-2 \cdot (\xi - \xi_{mps}) / L_{mps}) \quad (8)$$

where $\psi = e \cdot \left(U - U_{pl}\right) / k \cdot T_e$ is the normalized potential, ξ is the distance from the surface in units of the Debye length, $\psi_{mps} = \ln \cos \alpha$ is the normalized potential drop in the mps as derived in [4], α is an angle between the magnetic field and the surface normal, $L_{mps} = k \cdot \rho_{iCs} \cdot \sin \alpha$ is the length of the magnetic pre-sheath, the factor k can be chosen between 2 – 3 [1], ρ_{iCs} is the Larmor radius corresponding to the ion acoustic velocity in units of the Debye length, ξ_{mps} is the distance to the mps/DS boundary.

For the potential distribution in the DS, the approximation of the numerical solution to the Poisson equation derived in [1] with the boundary conditions at the surface (equation (7)) and at the DS/mps (equation (8)) can be taken as the following:

$$\psi(\xi) = \psi_w + Q - Q \cdot \exp(-a \cdot \xi - c \cdot \xi^2) \quad (9)$$

where ψ_w is the dimensionless target potential (equation (7)), parameters a and Q are derived in [1], the parameter c and ξ_{mps} were determined by numeric iterations. The resulting sheath electric field potential is in good agreement with the numerical solution of the integral Poisson equation in the DS. Figure 1 presents the influence of the SB on the potential profiles calculated using the suggested analytical expression given by equations (8) and (9). The potential changes so that both the potential drop and the length of the DS increase.

The suggested model can be easily applied for various experiment conditions. Figure 2 illustrates the influence of the SB voltage on the angular distributions of the impinging D^+ ions calculated using the suggested AE for different magnetic field intensities and angles. Two opposite trends in the shift of the mean ion impact angle with SB are revealed: the main trend is the decrease of the mean impact angle with biasing, although under strong magnetic fields and at grazing angles ($\xi_{mps} > \rho_{iCs} \cdot \sin \alpha$) the electric field influence on the ion impact angle becomes inessential and the mean angle increases.

Further, the influence of SB on the effective sputtering coefficient of Be by incident D ions was calculated by integrating the Eckstein formula [6] for the angle and energy distributions obtained above. In most cases the effective sputtering yield increases by a factor of 3 with increasing the SB up to 200 V. However, at high magnetic field intensities at grazing angles the yield rises up to 10 times due to the angular factor.

Journal of Physics: Conference Series **748** (2016) 012002 doi:10.1088/1742-6596/748/1/012002

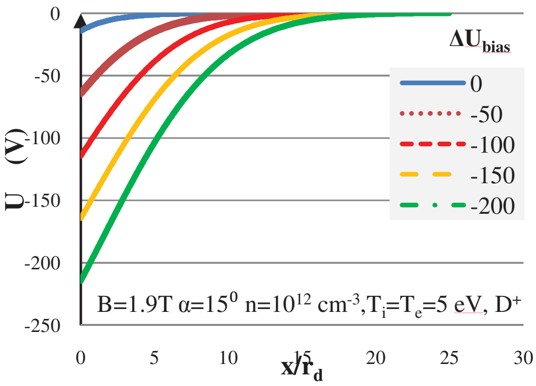

Figure 1. Potential profiles obtained using analytic expression (equations (8), (9)) for different biasing voltages.

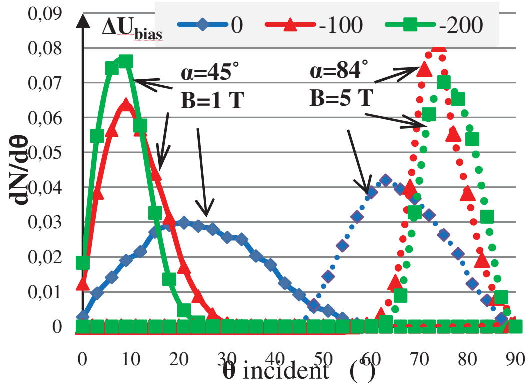

Figure 2. Surface biasing influence on the angular distributions of incident D ions for different values and angles of magnetic field to the surface (n=10^{12} cm^{-3}, T_i=T_e=5 eV).

3. Surface biasing influence on W target sputtering in the linear device PSI-2

The AE mentioned above was applied to the study of sputtering of the W target under Ar plasma exposure in PSI-2 linear plasma device [2]. Experimentally, the neutral W (400.9 nm) radiation intensity profiles were measured by a spectrometer along the normal distance to the target for various target voltages.

Using the expression (9) we calculated the energy and angular ion distributions and corresponding effective sputtering yield for each target voltage. In figure 3 the calculated data, normalised to the sputtering coefficient at $|U_t - U_{pl}|$ = 100V, are compared to the respective experimental data. The experimental values of the effective sputtering yield for each target voltage were obtained by integrating the W intensity profiles. The good agreement of simulated and experimental results proves the applicability of the suggested AE. The results obtained with the AE improve the estimates calculated using simplified sheath assumptions up to 10% in this particular case. However, the AE application efficiency increases with the ion temperature and magnetic field angle.

4. Simulation of enhanced by RF-emission erosion of JET Be limiter

The AE derived above has also been applied for modelling of 2-3 times enhanced erosion of the outer wall JET Be limiter modulated by toggling of ICRH RF-antenna 'C' [3]. This effect has been associated with magnetic connections between the affected PFCs and high electric fields induced by the antenna, the latter being represented in modeling by an additional negative SB of up to 200 V [7]. Figure 4 presents the sputtering coefficients in the assumption of the low-recycling plasma scenario calculated with the AE and obtained in the earlier simulations which did not account for the influence of the oblique magnetic field [3]. These sputtering coefficients were calculated assuming 50% D concentration in the surface interaction layer ('ERO-min') [8]. For comparison the case of a pure beryllium target ('ERO-max') was also calculated with the AE. It is shown that for 'ERO-min' fit, the calculated sputtering yield increases 2-3 times with biasing, which is in qualitative agreement with the experimental results (α=85.8°, B=1.9 T, n=10^{12} cm^{-3}, T_i=T_e=5eV). This provides additional confidence in 'ERO-min' fit for the physical sputtering yields for the plasma-wetted areas of PFCs. The properly treated angular factor in the sputtering yield leads to reproducing of the experimental erosion increase mentioned above.

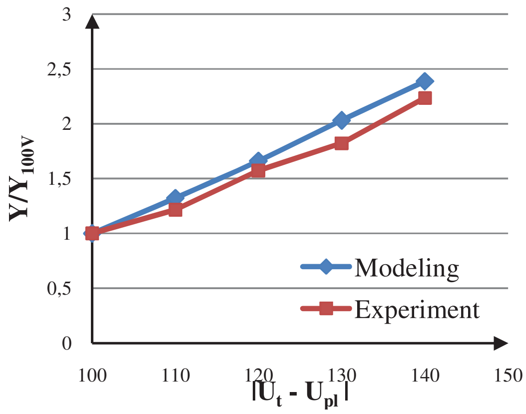

Figure 3. Comparison of the experimental and simulated dependences of the sputtering yields of W target by Ar ions impact on ion incident energy in the linear device PSI-2 (α=0°, B=0.1T, n = 0.45·10^{12} cm^{-3}, T_i = 1eV, T_e = 4eV, U_{pl} = -10V, Ar^+).

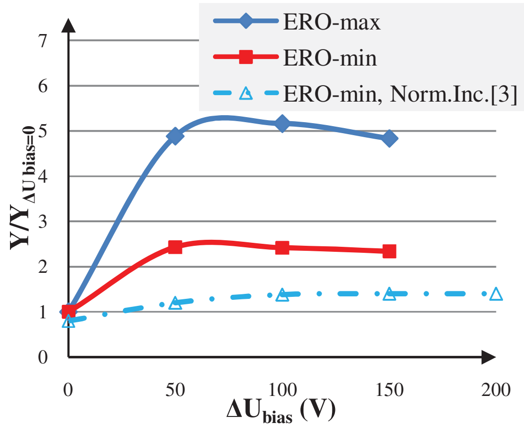

Figure 4. Comparison of the simulation with AE for different surface content, the earlier ERO modeling (ERO-min for normal incidence) and experimental observations (rectangle) of Be limiter erosion.

5. Conclusion

The simplified analytical expression for the electromagnetic field in the DS suggested in [1] is now updated to include surface biasing effect. The energy and angular impact distributions and surface sputtering yields were computed in the presence of an oblique magnetic field and surface biasing. Two opposite trends of the mean ion impact angle shift with surface biasing are revealed: in most cases, the mean impact angle decreases with biasing, however, under strong magnetic fields and at grazing angles the mean angle increases.

The AE was used to estimate the sputtering yield of the tungsten target under Ar plasma for various target voltages in PSI-2 experiments. The simulation and experimental results are in a good agreement. The same AE has been applied for improving earlier estimates [3] of enhanced by RF-emission erosion of the outer wall JET Be limiter near the ICRH antenna. It is shown that an additional negative surface biasing more than 50 V can explain the observed 2-3 fold increase in erosion (characterized by Be spectroscopy), assuming 50% D concentration in the surface interaction layer. The updated model, however, leads to an increased effect due to the synergy with the properly treated angular factor in the sputtering yield. This leads to a qualitative change in the results: for instance with the earlier model [3] the increase in erosion observed experimentally could not be reproduced under the low-recycling plasma assumption. In addition, the roughness of the substrates can influence the surface sputtering as is shown in [9]. Therefore, some of our earlier modeling results and conclusions for ERO modeling of enhanced by RF-emission erosion of the outer wall JET Be limiter near the ICRH antenna [5] should be re-visited.

Acknowledgements
This work has been initiated within the MEPhi – FZJ strategic partnership. The views and opinions expressed herein do not necessarily reflect those of the European Commission. The authors (I. Borodkina, I.V. Tsvetkov and V.A. Kurnaev) also would like to thank for the support from National Research Nuclear University MEPhI in the framework of the Russian Academic Excellence Project (contract No. 02.a03.21.0005, 27.08.2013).

References

[1] Borodkina I et al. PET-2015 submitted to *CPP*
[2] Eksaeva A et al. 2015 *Proc. of the XXII Int. Conf. ISI-2015* 82
[3] Klepper C C et al. 2016 *Phys. Scr.* 014035
[4] Stangeby P 2000 *The plasma boundary of magnetic fusion devices* (Plasma physics series) (London: IOP Publishing Ltd)
[5] Weinlich M, Carlson A 1997 *Phys.Plasmas* **4** **(6)** 2151
[6] Behrisch R, Eckstein W 2007 *Topics Appl. Physics* **110** 33
[7] Bobkov V V et al. 2010 *Nucl. Fusion* **50** 035004
[8] Borodin D et al. 2013 *J. Nucl. Mater.* **438** 267
[9] Shuyu D et al. 2015 *J. Nucl. Mater*. **463** 372